



Deposited via The University of Leeds.

White Rose Research Online URL for this paper:

<https://eprints.whiterose.ac.uk/id/eprint/186906/>

Version: Accepted Version

Proceedings Paper:

Zhao, Y, Dehghani-Sani, AA and Xie, S (2021) Electromyography-based Adaptive Cooperative Control for a Wrist Orthosis. In: 2021 27th International Conference on Mechatronics and Machine Vision in Practice (M2VIP). 2021 27th International Conference on Mechatronics and Machine Vision in Practice (M2VIP), 26-28 Nov 2021, Shanghai, China. IEEE. ISBN: 978-1-6654-3153-8.

<https://doi.org/10.1109/m2vip49856.2021.9665116>

© 2021, IEEE. Personal use of this material is permitted. Permission from IEEE must be obtained for all other uses, in any current or future media, including reprinting/republishing this material for advertising or promotional purposes, creating new collective works, for resale or redistribution to servers or lists, or reuse of any copyrighted component of this work in other works.

Reuse

Items deposited in White Rose Research Online are protected by copyright, with all rights reserved unless indicated otherwise. They may be downloaded and/or printed for private study, or other acts as permitted by national copyright laws. The publisher or other rights holders may allow further reproduction and re-use of the full text version. This is indicated by the licence information on the White Rose Research Online record for the item.

Takedown

If you consider content in White Rose Research Online to be in breach of UK law, please notify us by emailing eprints@whiterose.ac.uk including the URL of the record and the reason for the withdrawal request.

Electromyography-based Adaptive Cooperative Control for a Wrist Orthosis

Yihui Zhao, Abbas A. Dehghani-Sanij and Shengquan Xie

Abstract—This paper proposes an adaptive cooperative control method for a wrist orthosis, consisting of a trajectory tracking controller, an admittance controller integrated with an electromyography (EMG)-driven musculoskeletal model-based approach. The admittance controller adaptively alters the reference trajectory based on the estimated joint torque by the EMG-driven musculoskeletal model. The admittance parameters are regulated by accessing the wrist joint condition in real-time. Three experiments are conducted including, trajectory tracking control (TTC), fixed cooperative control (FCC), adaptive cooperative control (ACC) with two cooperative ratios of 0.3 and 0.6 respectively. Preliminary results demonstrate that the cooperative control strategies have smaller root-mean-square-errors compared with the TTC when the subject's intention is detected. The proposed method can modify the wrist orthosis's compliance in real-time in response to the wrist joint stiffness changes, which shows its potential to improve the efficiency and safety in rehabilitation.

I. INTRODUCTION

Rehabilitation robots hold promising advantages to deliver high-intensive and precise training scheme for stroke patients [1]–[3]. It has proven that the patient's active participation can improve the muscle function and neural-motor skills during robot-aided rehabilitation [4]. Estimation of the patient's intention and related control strategies have played important roles in interactive training schemes.

Electromyography (EMG) signal has been broadly adopted for estimating the patient's intention, due to the fact that neural pulse can be detected ahead of actual motion [5]. Major attentions of EMG-based intention estimation for upper limb rehabilitation are concerned with the regression methods, such as linear/non-linear regression [6] and NARX model [7]. Nevertheless, regression methods map EMG signal inputs to the desired intention through the numerical functions. However, the methods cannot describe the musculoskeletal states during motion tasks [8]. In contrast, musculoskeletal model-based approaches are alternative method for intention estimation. They explicitly interpret the relationships from the EMG signal to the user's intention by imitating the interactive effects among muscular and skeletal systems [9]. Besides, the underlying musculoskeletal states,

i.e., muscle force and joint stiffness, can be obtained from the model-based approaches [10]. These musculoskeletal states facilitate the design of the control strategies for interactive training schemes [11].

To provide the interactive training, impedance control and admittance control strategies are commonly utilized in rehabilitation robots. The impedance control strategy asks the robots to render particular mass, spring and damping properties to compensate for the torque generated by patients [12]. For example, Squeriet *et al.*, proposed an impedance controller for a wrist robot [13]. The impedance control scheme increases/decreases the supported torque by the robot as the patient's interactive torque decreases/increases. In this manner, the patient is encouraged to participate in the rehabilitation training. The admittance control is another control strategy used for the interactive training scheme, which provides the desired position according to patients' interaction torque. For instance, Chiaradia *et al.*, proposed an admittance control for a wrist exosuit, which generates the desired motion when the interaction torque is sensed [14]. However, the constant stiffness and damping parameters may limit the design of the interactive control strategies, as the joint condition changes varies patient to patient. The variation of these parameters in rehabilitation robots should take the patient's limb impedance property into account [15]. It was suggested that regulating these parameters according to the stiffness property of the joint can improve the performance of human-robot interaction [16]. Nevertheless, it is a challenging task to estimate the joint stiffness property, which is determined through experimental measurement of the torque-motion relationship under different maximum voluntary contraction [17]. The model-based approach provides a promising solution, in which the joint stiffness can be directly obtained by differentiating the model dynamic equations [10].

The aim of this paper is to develop an interactive training scheme for our a wrist orthosis developed by the intelligent Rehabilitation Robotics Center at Leeds [18]. The wrist orthosis is driven by two pneumatic muscles. To improve the training effectiveness and safety, an adaptive cooperative control strategy is developed. In this manner, the wrist orthosis adaptively alters the reference trajectory based on the estimated joint torque, in which the patient's intention (joint torque) is obtained directly by coupling the EMG-driven model-based approach. The admittance parameters are regulated to change the compliance of the wrist orthosis, depending on the real-time estimated joint stiffness. Three experiments are conducted to validate the performance of

Yihui Zhao is with the School of Electronic and Electrical Engineering, University of Leeds, Leeds LS2 9JT, U.K (e-mail: e114yz@leeds.ac.uk; e114kq@leeds.ac.uk).

Abbas A. Dehghani-Sanij is with the School of Mechanical Engineering, University of Leeds, Leeds LS2 9JT, U.K (email: A.A.Dehghani-Sanij@leeds.ac.uk).

Shengquan Xie is with the School of Electronic and Electrical Engineering, University of Leeds, Leeds LS2 9JT, U.K., also collaboration with the Institute of Rehabilitation Engineering, Binzhou Medical University, Yantai 264033, China. (email: s.q.xie@leeds.ac.uk)

the proposed control strategy, including trajectory tracking control (TTC), fixed cooperative control (FCC) and adaptive cooperative control (ACC) with two cooperative ratios (0.3 and 0.6 respectively).

II. METHODS

A. Wrist orthosis

The wrist orthosis [18] consists of two Festo Fluidic Muscles as the antagonistic actuators. Each muscle is attached to a mechanical hinge through a steel wire, of which the hinges are placed coaxial with the biological wrist joint. The wires are guided around the cylindrical hinges in clock/counter-clockwise setup and ball bearings are used to reduce the friction in the hinge. Two load cells are connected in series with the pneumatic muscles respectively. A potentiometer is utilized as an angle sensor, which is also aligned with rotation centre. Two proportional pressure regulators are used for pressure control of two muscles. EMG signal are collected through wireless electrodes (Delsys TrignoTM). All sensors are communicated with the NI-myRIO controller. A LabVIEW program is designed to process and store the sensing information and generate the desired trajectory for the wrist orthosis.

B. EMG-driven musculoskeletal model-based approach

The EMG-driven musculoskeletal model-based approach is used to compute the wrist flexion/extension joint torque. It transforms the muscle activities to the joint torque based on the input sEMG signal and joint angles during motion task, which comprises a muscle activation model, a muscle-tendon model and a musculoskeletal model. The EMG signal of four wrist muscles are recorded in this study ($i = 4$).

In the muscle activation model, the envelop of the sEMG signals are first obtained by filtering the raw signal using a 4th order Butterworth band-pass filter (pass band at 20 Hz and 450 Hz). The filtered signals are fully rectified and low-pass filtered by a 4th order Butterworth low-pass filter at a corner frequency of 4 Hz. The low-pass filtered signal are normalized by the maximum voluntary contraction, results the enveloped signal $e_i(t)$ between 0 and 1. Then a non-linear equation is used to obtain the muscle activation $a_i(t)$ from the enveloped signal, which can be written as [19]

$$a_i(t) = \frac{e^{Au_i(t)} - 1}{e^A - 1} \quad (1)$$

where A is the non-linear shape factor that has the range between 0.001 and -3.

The muscle-tendon model is modelled as an elastic tendon connected in series with a muscle fibre [20]. The muscle fibre contains the contractile element (CE) and parallel element (PE). The relationship between muscle fibre and tendon is written as

$$l_i^m = (l_i^{mt} - l_i^t) \cos^{-1} \phi_i \quad (2)$$

where l_i^m , l_i^{mt} and l_i^t represent the muscle fibre length, muscle-tendon length and tendon length. ϕ_i is the pennation

angle between muscle fibre and tendon. The tendon strain is omitted for real-time computation.

The muscle-tendon length l_i^{mt} is obtained by regressing equations according to upper limb model [21]. With the muscle activation $a_i(t)$ and states of the muscle-tendon length l_i^{mt} as inputs, the muscle-tendon force F_i^{mt} can be computed by the following equations

$$F_i^{mt} = (F_{CE,i} + F_{PE,i}) \cos \phi_i \quad (3)$$

$$F_{CE,i} = F_{o,i}^m f_a(\bar{l}_{i,a}^m) f(\bar{v}_i) a_i(t) \quad (4)$$

$$F_{PE,i} = F_{o,i}^m f_p(\bar{l}_i^m) \quad (5)$$

$$\phi_i = \sin^{-1} \left(\frac{l_{o,i}^m \sin \phi_{o,i}}{l_i^m} \right) \quad (6)$$

where $F_{CE,i}$ is the active force generated by the contractile element, which is the function of the active force-length relationship $f_a(\bar{l}_{i,a}^m)$ and force-velocity relationship $f(\bar{v}_i)$. In specific, $F_{o,i}^m$ is the maximum isometric force. $\bar{l}_{i,a}^m$ is normalization of muscle fibre length l_i^m with respect to the muscle activation and optimal muscle fibre length $l_{o,i}^m$, which is given as

$$\bar{l}_{i,a}^m = l_i^m / (l_{o,i}^m (\lambda(1 - a_i(t)) + 1)) \quad (7)$$

where λ is set to 0.15 [22],

The passive force $F_{PE,i}$ is generated by the PE in the muscle fibre. $f_p(\bar{l}_i^m)$ denotes the passive force-length relationship when the muscle fibre length exceeds $l_{o,i}^m$. \bar{l}_i^m is the normalization of muscle fibre length with respect to $l_{o,i}^m$. Pennation angle ϕ_i changes as the muscle contraction (Equation (6)). Furthermore, $f_a(\bar{l}_{i,a}^m)$, $f(\bar{v}_i)$ and $f_p(\bar{l}_i^m)$ are expressed as

$$f_a(\bar{l}_{i,a}^m) = e^{-(\bar{l}_{i,a}^m - 1)^2 k_0^{-1}} \quad (8)$$

$$f(\bar{v}_i) = \frac{0.1433}{0.1074 + \exp(-1.409 \sinh(3.2\bar{v}_i + 1.6))} \quad (9)$$

$$f_p(\bar{l}_i^m) = \frac{e^{10(\bar{l}_i^m - 1)}}{e^5} \quad (10)$$

where the coefficient k_0 is used to approximate the force-length relationship, which is set to 0.45 [23]. \bar{v}_i is the normalization of the muscle velocity v_i of the maximum velocity $v_{o,i}$, which is equal to $10 l_{o,i}^m / \text{sec}$ [20], of which v_i is the derivative of the muscle fibre length with respect to time.

Moment arm of each muscle is determined by the partial derivative of muscle-tendon length with respect to the wrist joint angle

$$r_i = \frac{\partial l_i^{mt}}{\partial \theta} \quad (11)$$

where r_i represents the moment arm of i th muscle with respect to the flexion/extension joint angle. Thus, the wrist joint torque can be computed by

$$\hat{\tau} = \sum_{i=1}^4 r_i F_i^{mt} \quad (12)$$

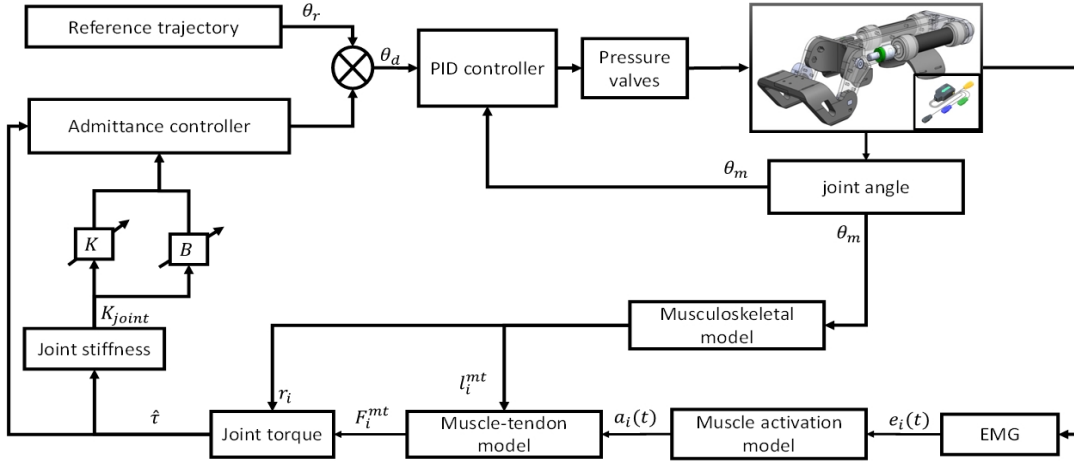


Fig. 1. The block diagram of the proposed adaptive cooperative control strategy for the wrist orthosis.

where $\hat{\tau}$ represents the estimated joint torque during motion task. The parameters in the muscle-tendon model that characterizes the properties of musculoskeletal system of each individual, including the optimal muscle fibre length $l_{o,i}^m$, tendon length l_i^t , maximum isometric force $F_{o,i}^m$ and optimal pennation angle $\phi_{o,i}$, the non-linear factor A and scale coefficient k_i . Thus, these parameters are optimized by the following objective function

$$f(\chi) = \frac{1}{N} \sum_{n=1}^N (\tau - \hat{\tau}) \quad (13)$$

$$\chi = [F_{o,i}^m, l_{o,i}^m, l_i^t, k_i, A]$$

where τ is the reference joint torque and $\hat{\tau}$ is the joint torque estimated by the musculoskeletal model-based approach. N represents the number of samples. Initial value of these parameters are assigned based on the upper limb extremity model [21]. The parameters are optimized by minimizing the objective function using genetic algorithm in MATLAB offline.

C. Adaptive cooperative control

To improve the training efficiency and engage participants in the rehabilitation, an admittance controller is developed to modify the reference trajectory according to the participant's active involvement [24]. The joint position and joint torque is defined as positive when wrist is flexed. The transfer function of the admittance controller is written as

$$\theta_d(s) = \theta_r(s) + \frac{C_r \hat{\tau}(s)}{Ms^2 + Bs + K} \quad (14)$$

where θ_d and θ_r are the desired trajectory and reference trajectory respectively. C_r is the cooperative ratio. $\hat{\tau}$ is the estimated joint torque from the sEMG signal. The M , B and K are the mass, damping and stiffness parameters of the admittance controller. As the wrist joint stiffness varies depending on the PE of muscle as well as active muscle activities. An adaptation method for the admittance

parameters is derived based on the estimated joint stiffness K_{joint} , which can be calculated by

$$K = -\frac{1}{2}K_{joint} + 10 \quad (15)$$

where joint stiffness K_{joint} is obtained by [10]

$$K_{joint} = \sum_{i=1}^4 (r_i^2 K_i^{mt} + \frac{\partial r_i}{\partial \theta} F_i^{mt}) \quad (16)$$

in which K_i^{mt} represents the stiffness of muscle-tendon model. It is modelled as the contractile element stiffness in parallel with stiffness of PE,

$$K_i^{mt} = K_i^{CE} + K_i^{PE} \quad (17)$$

and K_i^{CE} is equal to

$$K_i^{CE} = \frac{\gamma a_i(t) F_{o,i}^m f_a(\bar{l}_{i,a}^m)}{l_{o,i}^m} \quad (18)$$

where γ is set to 23.4 [25]. The K_i^{PE} is calculated by the slope of the passive force-length relationship to account for the muscle fibre stiffness in absence of the muscle activation $a_i(t)$ [10]. The damping parameter B is determined by [16]

$$B = 0.2\sqrt{K}. \quad (19)$$

A boundaries function of the stiffness parameter K is used to prevent the instability of the control system, where the K_{max} and K_{min} are set based on the measurement. Fig. 1 illustrates a block diagram of the proposed adaptive cooperative control strategy. With a predefined reference trajectory, the wrist orthosis operates in passive training mode when no subject's intentions are detected, whereas the reference trajectory is altered when the subject's intentions are measured. The admittance parameters are regulated according to estimated joint impedance property in real-time.

III. EXPERIMENT

Three healthy subjects (S1-S3) have participated in this test in the lab environment. All subjects have no wrist muscular disorder and can perform the wrist flexion/extension in full range of motion (RoM). During the experiment, the subject is asked to wear the wrist orthosis. Electrodes are attached over four wrist primary muscles, including Flexor Carpi Radialis (FCR), Flexor Carpi Ulnaris (FCU), Extensor Carpi Radialis Longus (ECRL), Extensor Carpi Radialis Brevis (ECRB). The placement of electrodes are according SENIAM recommendation and palpation [26]. The processed EMG signals are downsampled to 200 Hz. All sensor data are synchronized and stored in customized LabVIEW program for offline analysis.

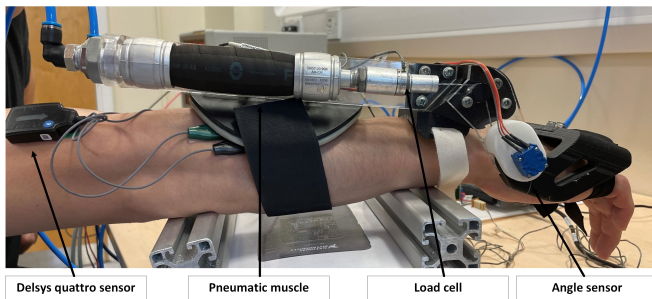


Fig. 2. Experiment setup.

To validate the performance of the proposed adaptive cooperative control strategy, three experiments, namely, trajectory tracking control (TTC), fixed cooperative control (FCC), adaptive cooperative control (ACC) with two different cooperative ratios are conducted for each subject. The cooperative control strategies can be used in both passive and active training exercise, i.e., wrist orthosis is under passive mode if there is no active torque and switch to the cooperative control model when muscle activities are detected [27]. In all experiments, the reference trajectory is set as a sine-wave with the amplitude of 0.25 rad and frequency of 0.05 Hz.

The first experiment (TTC) is conducted without the cooperative control strategy. A proportional-integral (PI) controller is implemented to minimize the tracking errors, in which the parameters of the PI controller are tuned to 4.55 and 0.0105 for the K_P and K_I respectively. The second experiment (FCC) is conducted with the fixed admittance parameters, where the M , K and B are set to 0.15, 10 and 0.63. The cooperative ratio is set to 0.6 in FCC. The desired trajectory is determined by the estimated joint torque only. Lastly, the third experiment (ACC) is used to validate that the proposed adaptive control strategy is able to change the robot's compliance. The admittance parameters (K and B) are regulated according to equation (16) and (19) respectively. In addition, two cooperative ratios, 0.3 and 0.6 are set in the ACC.

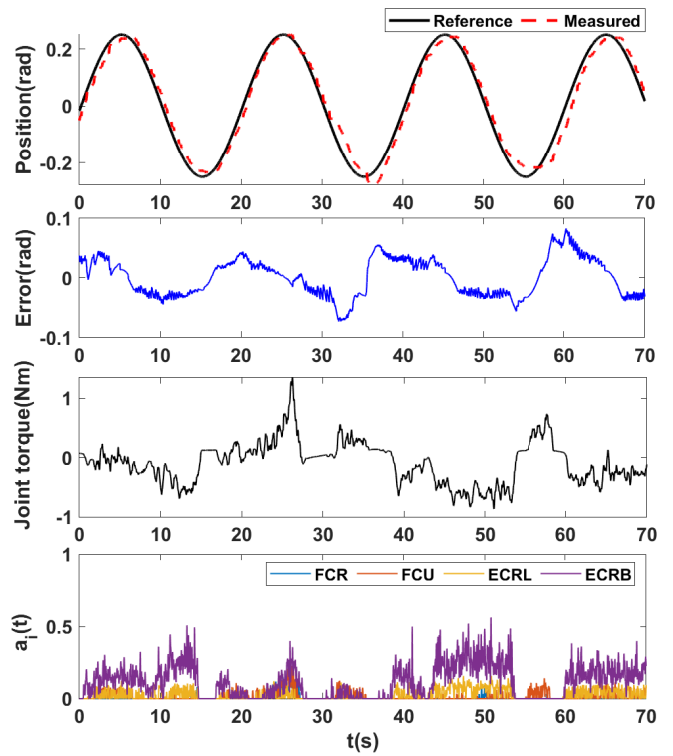


Fig. 3. Representative example of the tracking performance in the TTC.

IV. RESULTS AND DISCUSSION

In this study, three performance indexes are utilized. The root-mean-square-error ($rmse$) between the desired trajectory (reference trajectory for TTC) and measured trajectory is calculated. The root-mean-square of estimated joint torque (rms_{τ}) and the deviation (rms_{dev}) between the desired trajectory and reference trajectory are calculated to evaluate the performance of cooperative control strategies.

Fig 3 shows one representative example of the trajectory tracking response for the TTC over 70 seconds training, along with the estimated joint torque and muscle activations $a_i(t)$. In the top figure, the black solid line indicates the reference trajectory and the red dotted line is the measured trajectory. The $rmse$ is 0.0314 rad. The result shows that the measured trajectory deviates significantly when the subject's intention is presented. This is caused by the backdrivability of the wrist orthosis, which ensures safety in rehabilitation but leads to more tracking errors [28]. Moreover, it may cause discomfort or injury to the wrist joint if the robot still follows the reference trajectory.

The representative example of tracking response for the second experiment (FCC) is shown in Fig 4. The green line represents the desired trajectory which is generated according to the estimated joint torque. The $rmse$ between the desired trajectory and measured trajectory is 0.0273 rad. The rms_{τ} and rms_{dev} are 0.3693 Nm and 0.0216 rad, respectively. In the FCC, the deviation of the reference trajectory is in line with the estimated joint torque. For instance, in the span of 30 seconds and 50 seconds, the wrist orthosis gives

TABLE I

$rmse$ (rad), rms_{τ} (Nm) AND rms_{dev} (rad) FOR ALL EXPERIMENTS AND ACROSS ALL SUBJECTS. TTC = Trajectory tracking control; FCC = Fixed cooperative control; ACC = Adaptive cooperative control; C_r = Cooperative ratio.

| | TTC | | FCC ($C_r = 0.6$) | | | ACC ($C_r = 0.3$) | | | ACC ($C_r = 0.6$) | | |
|-------------|--------|--------------|---------------------|--------------|-------------|---------------------|--------------|-------------|---------------------|--------------|-------------|
| | $rmse$ | rms_{τ} | $rmse$ | rms_{τ} | rms_{dev} | $rmse$ | rms_{τ} | rms_{dev} | $rmse$ | rms_{τ} | rms_{dev} |
| S1 | 0.031 | 0.356 | 0.027 | 0.369 | 0.022 | 0.027 | 0.488 | 0.023 | 0.032 | 0.443 | 0.029 |
| S2 | 0.038 | 0.169 | 0.026 | 0.371 | 0.022 | 0.029 | 0.588 | 0.020 | 0.029 | 0.350 | 0.024 |
| S3 | 0.037 | 0.118 | 0.029 | 0.248 | 0.015 | 0.023 | 0.328 | 0.016 | 0.030 | 0.318 | 0.026 |
| Mean | 0.035 | 0.214 | 0.028 | 0.329 | 0.020 | 0.026 | 0.468 | 0.020 | 0.030 | 0.371 | 0.026 |
| std | 0.004 | 0.125 | 0.001 | 0.07 | 0.004 | 0.003 | 0.131 | 0.004 | 0.001 | 0.065 | 0.003 |

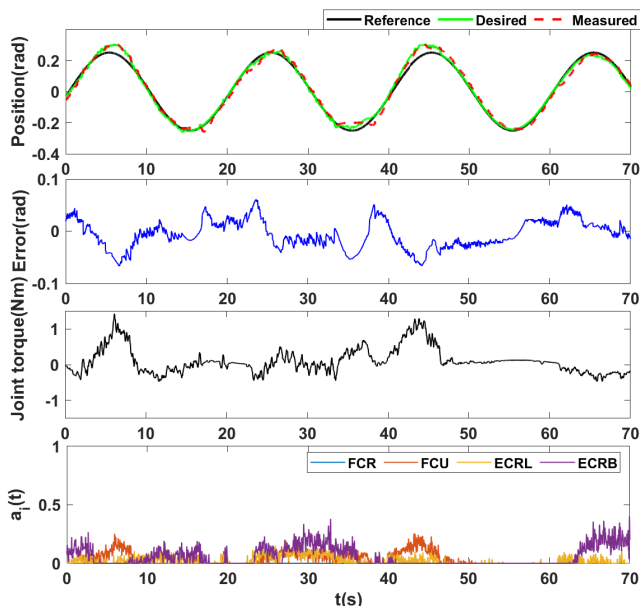


Fig. 4. Representative example of tracking response in the FCC. The M , K and B are set to 0.15, 10 and 0.63 in admittance controller.

more RoM toward wrist flexion when the joint torque is positive. Furthermore, the robot reduces the RoM in the extension as the joint torque is positive between 50 seconds and 60 seconds.

Fig 5 and Fig 6 illustrate the tracking responses of the ACC with two different cooperative ratios for the representative subject. The $rmse$ are 0.027 rad and 0.0317 rad when the cooperative ratio is set to 0.3 and 0.6 respectively. In addition, the real-time changes of admittance parameters are also presented. Results show that the robot can measure the subject's intention. The robot modifies the reference trajectory when the admittance parameters are small in both cases. For instance, at 40 seconds of fig 6, the reference trajectory deviates more in extension when the admittance parameters are small. In addition, it shows the robot's compliance is influenced by the co-contraction of the wrist muscles. For example, in Fig 5, the stiffness and damping are large between 10 and 20 seconds when wrist extensors are activated. The stiffness is small in the span of 30 and 40 seconds due to the co-contraction of wrist muscle.

Table I summarises the performance indexes of four experiments for all three subjects. Preliminary results show that the

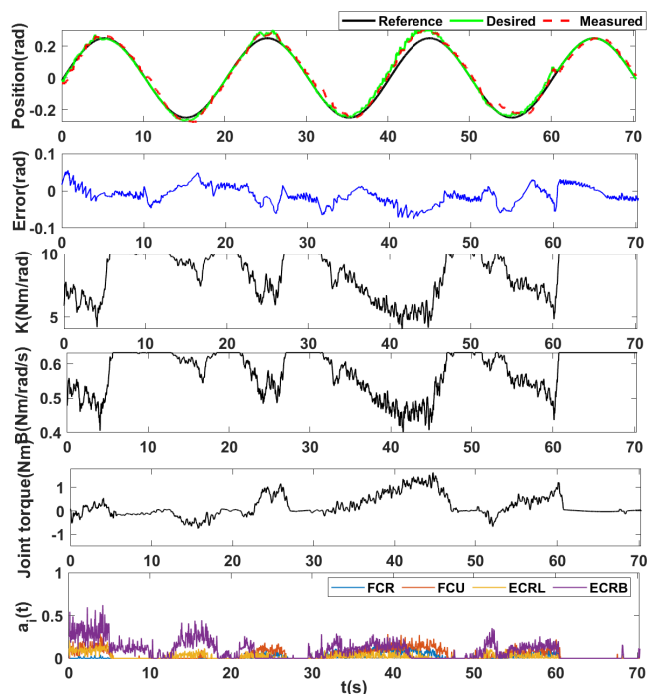


Fig. 5. Representative example of tracking response in ACC with 0.3 C_r .

cooperative control strategies improve training safety. This is because that the mean $rmse$ of TTC (0.035 rad) is larger than FCC and ACC, while the rms_{τ} is smaller (0.214 Nm). This indicates that the cooperative control strategies have the capability to follow the subject's intention. The cooperative ratio is introduced to scale the compliance of the wrist orthosis. The mean rms_{τ} of 0.3 C_r is larger than 0.6 C_r , but results in smaller rms_{dev} . This indicates that the wrist orthosis can more easily change the wrist orthosis's compliance with higher C_r . For the FCC and ACC with 0.6 C_r , both control strategies have similar performance indexes. Further studies will recruit more subjects, including stroke patients, to provide the statistical analysis.

V. CONCLUSION

In this paper, an adaptive cooperative control strategy incorporating the EMG-driven musculoskeletal model is implemented for the pneumatic-driven wrist orthosis to improve training effectiveness and safety. The EMG model-based approach is used to compute the joint torque in FCC and ACC,

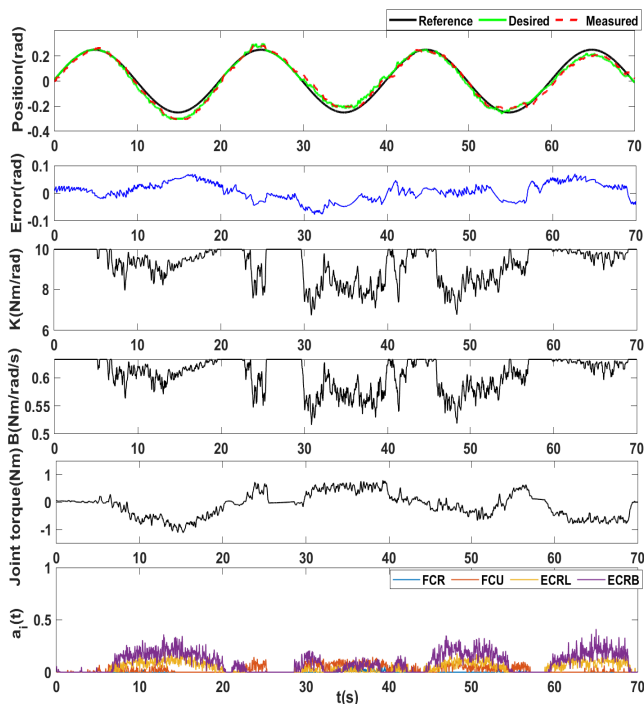


Fig. 6. Representative example of tracking response in ACC with $0.6 C_T$.

while the joint stiffness is used to regulate the admittance parameters in ACC.

Preliminary results demonstrate that FCC and ACC can improve safety when the subject's intention takes place. TTC has higher $rmse$ and lower rms_τ than cooperative control strategies. Meanwhile, the proposed ACC has shown the capability to adjust the wrist orthosis's compliance in real-time by accessing the wrist joint stiffness through the musculoskeletal model-based approach. The results show the potential to enhance the efficacy and safety of robot-assisted therapy. Future studies will be carried out on more subjects, including stroke patients, to obtain the statistical analysis.

REFERENCES

- [1] P. Maciejasz, J. Eschweiler, K. Gerlach-Hahn, A. Jansen-Troy, and S. Leonhardt, "A survey on robotic devices for upper limb rehabilitation," *J Neuroeng Rehabil*, vol. 11, no. 1, pp. 1–29, 2014.
- [2] S. Hussain, P. K. Jamwal, P. Van Vliet, and M. H. Ghayesh, "State-of-the-art robotic devices for wrist rehabilitation: Design and control aspects," *IEEE Trans Hum Mach Syst*, vol. 50, no. 5, pp. 361–372, 2020.
- [3] P. Langhorne, J. Bernhardt, and G. Kwakkel, "Stroke rehabilitation," *The Lancet*, vol. 377, no. 9778, pp. 1693–1702, 2011.
- [4] V. R. Edgerton and R. R. Roy, "Robotic training and spinal cord plasticity," *Brain research bulletin*, vol. 78, no. 1, pp. 4–12, 2009.
- [5] P. R. Cavanagh and P. V. Komi, "Electromechanical delay in human skeletal muscle under concentric and eccentric contractions," *Eur. J. Appl. Physiol.*, vol. 42, no. 3, pp. 159–163, 1979.
- [6] J. Liu, Y. Ren, D. Xu, S. H. Kang, and L.-Q. Zhang, "EMG-based real-time linear-nonlinear cascade regression decoding of shoulder, elbow, and wrist movements in able-bodied persons and stroke survivors," *IEEE Trans. Biomed. Eng.*, vol. 67, no. 5, pp. 1272–1281, 2019.
- [7] J. Liu, S. H. Kang, D. Xu, Y. Ren, S. J. Lee, and L.-Q. Zhang, "EMG-based continuous and simultaneous estimation of arm kinematics in able-bodied individuals and stroke survivors," *Front. Neurosci.*, vol. 11, p. 480, 2017.

- [8] M. Sartori, D. G. Lloyd, and D. Farina, "Neural data-driven musculoskeletal modeling for personalized neurorehabilitation technologies," *IEEE Trans. Biomed. Eng.*, vol. 63, no. 5, pp. 879–893, 2016.
- [9] N. Lotti, M. Xiloyannis, G. Durandau, E. Galofaro, V. Sanguineti, L. Masia, and M. Sartori, "Adaptive model-based myoelectric control for a soft wearable arm exosuit: A new generation of wearable robot control," *IEEE Robot Autom Mag*, vol. 27, no. 1, pp. 43–53, 2020.
- [10] A. Zonnino and F. Sergi, "Model-based analysis of the stiffness of the wrist joint in active and passive conditions," *J. Biomech. Eng.*, vol. 141, no. 4, 2019.
- [11] M. G. Carmichael and D. Liu, "Estimating physical assistance need using a musculoskeletal model," *IEEE Trans. Biomed. Eng.*, vol. 60, no. 7, pp. 1912–1919, 2013.
- [12] K. M. Lynch and F. C. Park, *Modern Robotics*. Cambridge University Press, 2017.
- [13] V. Squeri, L. Masia, P. Giannoni, G. Sandini, and P. Morasso, "Wrist rehabilitation in chronic stroke patients by means of adaptive, progressive robot-aided therapy," *IEEE Trans. Neural Syst. Rehab. Eng.*, vol. 22, no. 2, pp. 312–325, 2013.
- [14] D. Chiaradia, L. Tiseni, M. Xiloyannis, M. Solazzi, L. Masia, and A. Frisoli, "An assistive soft wrist exosuit for flexion movements with an ergonomic reinforced glove," *Front. Robot. AI*, vol. 7, p. 182, 2021.
- [15] M. Sharifi, A. Zakerimanesh, J. K. Mehr, A. Torabi, V. K. Mushahwar, and M. Tavakoli, "Impedance variation and learning strategies in human-robot interaction," *IEEE Trans Cybern*, pp. 1–14, 2021.
- [16] P. Liang, C. Yang, Z. Li, and R. Li, "Writing skills transfer from human to robot using stiffness extracted from SEMG," in *2015 IEEE 7th Annu. Int. Conf. CYBER Technol.* IEEE, 2015, pp. 19–24.
- [17] A. B. Leger and T. E. Milner, "Passive and active wrist joint stiffness following eccentric exercise," *Eur. J. Appl. Physiol.*, vol. 82, no. 5, pp. 472–479, 2000.
- [18] W. Meng, B. Sheng, M. Klinger, Q. Liu, Z. Zhou, and S. Q. Xie, "Design and control of a robotic wrist orthosis for joint rehabilitation," in *2015 IEEE/ASME Int. Conf. Adv. Intell. Mechatron. AIM.* IEEE, 2015, pp. 1235–1240.
- [19] T. S. Buchanan, D. G. Lloyd, K. Manal, and T. F. Besier, "Neuromusculoskeletal modeling: estimation of muscle forces and joint moments and movements from measurements of neural command," *J. Appl. Biomech.*, vol. 20, no. 4, pp. 367–395, 2004.
- [20] F. E. Zajac, "Muscle and tendon: properties, models, scaling, and application to biomechanics and motor control," *Crit Rev Biomed Eng*, vol. 17, no. 4, pp. 359–411, 1989.
- [21] K. R. Saul, X. Hu, C. M. Goehler, M. E. Vidt, M. Daly, A. Velisar, and W. M. Murray, "Benchmarking of dynamic simulation predictions in two software platforms using an upper limb musculoskeletal model," *Comput Methods Biomech Biomed Engin*, vol. 18, no. 13, pp. 1445–1458, 2015.
- [22] D. G. Lloyd and T. F. Besier, "An EMG-driven musculoskeletal model to estimate muscle forces and knee joint moments in vivo," *J. Biomech.*, vol. 36, no. 6, pp. 765–776, 2003.
- [23] D. G. Thelen, "Adjustment of muscle mechanics model parameters to simulate dynamic contractions in older adults," *J. Biomech. Eng.*, vol. 125, no. 1, pp. 70–77, 2003.
- [24] D. Xu, M. Zhang, H. Xu, J. Fu, X. Li, and S. Q. Xie, "Interactive compliance control of a wrist rehabilitation device (WReD) with enhanced training safety," *J. Healthc. Eng.*, vol. 2019, 2019.
- [25] L. Cui, E. J. Perreault, H. Maas, and T. G. Sandercock, "Modeling short-range stiffness of feline lower hindlimb muscles," *J. Biomech.*, vol. 41, no. 9, pp. 1945–1952, 2008.
- [26] H. J. Hermens, B. Freriks, R. Merletti, D. Stegeman, J. Blok, G. Rau, C. Disselhorst-Klug, and G. Hägg, "European recommendations for surface electromyography," *Roessingh research and development*, vol. 8, no. 2, pp. 13–54, 1999.
- [27] M. Zhang, S. Q. Xie, X. Li, G. Zhu, W. Meng, X. Huang, and A. J. Veale, "Adaptive patient-cooperative control of a compliant ankle rehabilitation robot (carr) with enhanced training safety," *IEEE Trans. Ind. Electron.*, vol. 65, no. 2, pp. 1398–1407, 2017.
- [28] P. Jamwal, "Design analysis and control of wearable ankle rehabilitation robot," Ph.D. dissertation, ResearchSpace@ Auckland, 2011.